Chelation Kinetics of Bidentate Phosphine Ligands on Pentacoordinate Ruthenium Carbonyl Complexes

Kevin A. Bunten, David H. Farrar,* Anthony J. Poë,* and Alan J. Lough

Department of Chemistry, University of Toronto, Lash Miller Chemistry Laboratories, 80 St. George Street, Toronto, Ontario, Canada, M5S 3H6

Received April 5, 2000

Chelation kinetics of the complexes $Ru(CO)_4(\eta^1\text{-}(P-P))$ have been studied in heptane, where P−P = $Ph_2P(CH_2)_nPPh_2$ (n = 1, 2, 3, or 4, i.e., dppm, dppe, dppp, or dppb), $Ph_2P(NMe)PPh_2$ (dppma), $Ph_2P(o\text{-}C_6H_4)PPh_2$ (dpp-benzene), or $R_2P(CH_2)_2PR_2$ (R = Me or Cy, i.e., dmpe or dcpe). The complexes were prepared in situ by reaction of the bidentate ligands with $Ru(CO)_4(C_2H_4)$, which itself was prepared in situ by photolysis of $Ru_3(CO)_{12}$ under C_2H_4. The initially formed $Ru(CO)_4(\eta^1\text{-}(P-P))$ complexes react cleanly to form axial−equatorial $Ru(CO)_3(\eta^2\text{-}(P-P))$, as shown by the crystallographic structures of the products when P−P = dppe, dmpe, and dpp-benzene and the close similarity of their FTIR spectra to those of the other products. The chelated products undergo further reaction in solution or the solid state, and the product when P−P = dppma has been characterized by crystallography as $Ru_2(CO)_3(\mu\text{-}PPh_2)(\mu\text{-}Ph_2PNMePPh_2)$. The kinetics of the displacement of CO from $Ru(CO)_4(\eta^1\text{-}(P-P))$ in *n*-heptane are characterized by $\Delta H^{\ddagger}$ values that are lower by up to 9 kcal mol^{-1} than those of their monodentate P-donor analogues. $\Delta S^{\ddagger}$ values range from quite positive to slightly negative and suggest a trend from purely dissociative to appreciably associative mechanisms along the series P−P = dpp-benzene < dcpe < dmpe < dppp ≤ dppm ≈ dppbu ≈ dppe ≪ dppma. This contrasts with the CO-dissociative reactions of analogous $Ru(CO)_4L$ complexes when L = monodentate P-donor ligands.

Introduction

Organometallic carbonyl compounds are widely used as hydrogenation and hydroformylation catalysts.[1] An important step in many catalytic cycles involves dissociation of a carbonyl ligand from the metal center so as to create a vacant coordination site at which rapid reactions can occur.[2] Kinetic studies of this process can shed light on the efficiency of such reactions, and many studies of CO dissociation from six-coordinate d^6 metal carbonyls have been reported.[2,3] The size[2a,g,3,4] of any substituent ancillary ligands often has a significant influence on their reaction rates. Kinetic studies of CO dissociation from five-coordinate metal carbonyls are still quite rare,[2,3] but displacement of CO from $Ru(CO)_4(L)$ (L = P-donor and some other ligands) has received detailed study (eq 1). The reactions are solely CO-dissociative, are significantly sensitive to the size of the substituents, L, and are characterized by high positive values of $\Delta S^{\ddagger}$.[4]

$$Ru(CO)_4L + L \xrightarrow{\triangle} Ru(CO)_3L_2 + CO \qquad (1)$$

Because P-donor ligands have a wide range of electronic and steric properties, the effectiveness of metal carbonyl catalysts can be greatly influenced by their presence as substituents,[5] and there is a consequent possibility of "tuning" catalysts by selection of appropriate ligands. One distinctive class of ligands is made up of polydentate phosphorus donors. They have been used to stabilize cluster complexes against fragmentation,[6] and, when used in mononuclear carbonyls, they have been shown to exhibit exceptional behavior. For instance, Gladfelter et al.[5] demonstrated that a chelating ligand made neutral ruthenium and iron complexes easier to oxidize and the corresponding products are more reactive than their nonchelated counterparts. A very important application for chelating phosphines is their use as ligands in transition metal catalyzed synthesis of chiral organic compounds.[7]

The actual process of forming chelate complexes of bidentate phosphine ligands has received relatively little attention in organometallic chemistry. In the 1970s, Connor et al.[8] demonstrated that chelation reactions of bidentate phosphines on metal carbonyls of group VI (Cr, Mo, and W) proceed with varying degrees of bond making and bond breaking in the transition state,

(1) (a) Cotton, F. A.; Wilkinson, G. In *Advanced Inorganic Chemistry*, 5th ed.; Wiley: New York, 1988. (b) Tkatchenko, I. In *Comprehensive Organometallic Chemistry*; Wilkinson, G., Stone, F. G. A., Abel, E. W., Eds.; Pergamon: Oxford, 1982; Vol. 8, pp 101−223. (c) Feng, J.; Garland, M. *Organometallics* **1999**, *18*, 417.

(2) (a) Howell, J. A. S.; Burkinshaw, P. M. *Chem. Rev.* **1983**, *83*, 557. (b) Agbosoou, F.; Carpentier, J.-F.; Mortreux, A. *Chem. Rev.* **1995**, *95*, 2485. (c) Schmid, R.; Hermann, W. A.; Fenking, G. *Organometallics* **1997**, *16*, 701. (d) Atwood, J. D.; Brown, T. L. *J. Am. Chem. Soc.* **1976**, *98*, 3155. (e) Angelici, R. J.; Basolo, F. *J. Am. Chem. Soc.* **1962**, *84*, 2495. (f) Graham, J. R.; Angelici, R. J. *Inorg. Chem.* **1967**, *6*, 2082. (g) Angelici, R. J.; Basolo, F. *Inorg. Chem.* **1963**, *2*, 728.

(3) Basolo, F. *Polyhedron* **1990**, *9*, 1503.

(4) (a) Chen, L.; Poë, A. J. *Inorg. Chem.* **1989**, *28*, 3641. (b) Poë, A. J.; Twigg, M. V. *Inorg. Chem.* **1974**, *13*, 2982. (c) Johnson, B. F. G.; Lewis, J.; Twigg, M. V. *J. Chem. Soc., Dalton Trans.* **1975**, 1876.

(5) (a) Sherlock, S. J.; Boyd, D. C.; Moasser, B.; Gladfelter, W. L. *Inorg. Chem.* **1991**, *30*, 3636. (b) Moasser, B.; Gross, C.; Gladfelter, W. L. *J. Organomet. Chem.* **1994**, *471*, 201.

(6) Bahsoun, A. A.; Osborn, J. A.; Voelker, C.; Bonnet, J. J.; Lavigne, G. *Organometallics* **1982**, *1*, 1114.

10.1021/om000289t CCC: $19.00
Publication on Web 08/10/2000

depending on the chelating ligand (eq 2). Recently, the kinetics of ring closure reactions of bidentate nitrogen[9] and sulfur[10] ligands were studied in detail. All of these reactions involve six-coordinate octahedral complexes, and no studies of chelating phosphine ligands on five-coordinate complexes have been reported.

$$M(CO)_5(\eta^1\text{-}(P-P)) \xrightarrow{\triangle} M(CO)_4(\eta^2\text{-}(P-P)) + CO \quad (2)$$

$$Ru(CO)_4(\eta^1\text{-}(P-P)) \xrightarrow{\triangle} Ru(CO)_3(\eta^2\text{-}(P-P)) + CO \quad (3)$$

We have studied the formation of $Ru(CO)_3(\eta^2\text{-}(P-P))$ from $Ru(CO)_4(\eta^1\text{-}(P-P))$ (eq 3) with a variety of chelating diphosphines so as to observe whether the presence of bidentate phosphine ligands with one P-donor atom already tethered to the metal will introduce some degree of bond making into the transition state for introduction of the second P-donor atom. An enhancement of the associative mechanism, not evident in the reactions shown in eq 1, could occur as a result of the high "local concentrations" of the initially nonbonded P-donor atom. Thorough study of entropies of reaction ($\Delta S^{\ddagger}$) and volumes of activation ($\Delta V^{\ddagger}$) have demonstrated that chelation reactions of bidentate nitrogen compounds on group six metal carbonyls also proceed via varying degrees of bond making and bond breaking in the transition state.[9] This work confirms the validity of $\Delta S^{\ddagger}$ measurements as an effective indication of the intimate reaction mechanism. Negative values of $\Delta S^{\ddagger}$ have been taken to suggest an associative mechanism for the formation of $Os_3(CO)_{10}(\mu\text{-dppm})$ from $Os_3(CO)_{11}(\eta^1\text{-dppm})$.[11]

The results presented in this paper represent the first reported examples of chelation reactions of diphosphine ligands on pentacoordinate carbonyls where associative reactions might be favored for steric reasons.

Experimental Section

All chemical manipulations were carried out under an atmosphere of nitrogen using standard Schlenk techniques[12] unless otherwise stated. Triruthenium dodecacarbonyl (Strem) was recrystallized from dichloromethane before use. Solvents *n*-heptane (Caledon), hexanes (Uniscience), toluene (Uniscience), and pentane (Caledon) were distilled over sodium under a nitrogen atmosphere. Dichloromethane (Analchemia) was predried over $CaCl_2$ and distilled over P_2O_5 under nitrogen. Solid phosphine ligands (Digital Specialty Chemicals) bis(diphenylphosphino)methane, dppm (**a**); bis(diphenylphosphino)ethane, dppe (**b**); bis(diphenylphosphino)propane, dppp (**c**); and bis(diphenylphosphino)butane, dppbu (**d**) were recrystallized from ethanol. Bis(diphenylphosphino)methylamine, dppma (**g**), was provided by Dr. R. A. Burrow (University of Toronto).

o-Bis(diphenylphosphino)(benzene), dpp-benzene (**h**), and bis(dicyclohexylphosphino)ethane, dcpe (**f**) (Strem), were recrystallized from toluene before use. Liquid bis(dimethylphosphino)ethane, dmpe (**e**) (Strem), was used as received. Phosphine purity was determined by $^{31}P\{^1H\}$ NMR spectroscopy. Ethylene (99.5%) and carbon monoxide (99.5%) (BOC) were used as received. Nitrogen (BOC) was passed through a Driright column to remove moisture. Phosphorus NMR spectra were recorded on a Varian 300 MHz spectrometer, and chemical shifts were referenced to H_3PO_4 internal standard. Mass spectrometry data were collected on a Micromass 70S-250 mass spectrometer in EI mode using 70 eV electrons. X-ray data were collected on a Nonius Kappa CCD diffractometer using graphite-monochromated Mo Kα radiation ($\lambda = 0.71073$ Å). A combination of 1° phi and omega (with kappa offsets) scans were used to collect sufficient data. The data frames were integrated and scaled using the Denzo-SMN package.[13] The structures were solved and refined on F^2 using the SHELXTL\PC V5.03 package.[14]

Monodentate complexes $Ru(CO)_4(\eta^1\text{-}(P-P))$ (**1**(**a**−**h**)) are readily prepared in situ by reaction of an excess of bidentate phosphine ligand (**a**−**h**) with $Ru(CO)_4(C_2H_4)$ generated by photolysis of an *n*-heptane solution of $Ru_3(CO)_{12}$ under an atmosphere of ethylene (Scheme 1).[15]

Infrared spectra were recorded on a Nicolet 550 Magna FTIR spectrophotometer in absorbance mode. Kinetic studies involving air-stable ligands were performed by monitoring FTIR spectroscopic changes of *n*-heptane solutions of monodentate complexes in a temperature-controlled infrared cell (Wilmad Glass) equipped with NaCl windows and a 2 mm cell path-length. Reactions involving the air-sensitive ligands dmpe and dcpe were conducted under nitrogen in a Schlenk tube equipped with a rubber septum cap to allow sample removal

Scheme 1. Synthetic Route to Chelate Compounds and Decomposition Products

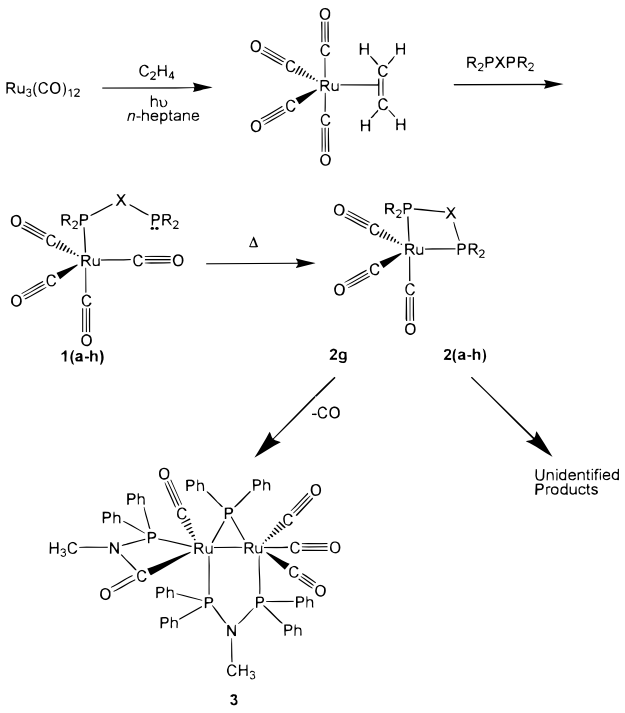

(7) (a) Procter, G. *Asymmetric Synthesis*; Oxford University Press: Oxford, 1996. (b) Noyori, R. *Asymmetric Catalysis In Organic Synthesis*; Wiley: New York, 1994.

(8) (a) Connor, J. A.; Day, J. P.; Jones, E. M.; McEwen, G. K. *J. Chem. Soc., Dalton Trans.* **1973**, 347. (b) Connor, J. A.; Riley, P. I. *J. Organomet. Chem.* **1975**, *94*, 55.

(9) (a) Dücker-Benfer, C.; Grevels, F.-W.; van Eldik, R. *Organometallics* **1998**, *17*, 1669. (b) Bal Reddy, K.; Brady, R. B.; Eyring, E. M.; van Eldik, R. *J. Organomet. Chem.* **1992**, *440*, 113. (c) Bal Reddy, K.; Hoffmann, R.; Konya, G.; van Eldik, R.; Eyring, E. M. *Organometallics* **1992**, *11*, 2319. (d) Zhang, S.; Zang, V.; Dobson, G. R.; van Eldik, R. *Inorg. Chem.* **1991**, *30*, 355. (e) Schneider, K. J.; van Eldik, R. *Organometallics* **1990**, *9*, 1235.

(10) Zang, S.; Dobson, G. R. *Inorg. Chem.* **1990**, *29*, 598.

(11) Poë, A. J.; Sekhar, V. C. *J. Am. Chem. Soc.* **1984**, *106*, 5034.

(12) Shriver, D. F.; Drezdzon, M. A. *The Manipulation of Air-Sensitive Compounds*, 2nd ed.; Wiley: New York, 1986.

(13) Otwinowski, Z.; Minor, W. *Methods Enzymol.* **1997**, *276*, 307.

(14) Sheldrick, G. M. *SHELXTL/PC V5.1*; Bruker Analytical X-ray Systems: Madison, WI, 1997.

(15) (a) Johnson, B. F. G.; Lewis, J.; Twigg, M. V. *J. Organomet. Chem.* **1974**, *67*, C75. (b) Chen, L.; Poë, A. J. *Inorg. Chim. Acta* **1995**, *240*, 399.

by means of a gastight syringe with a stainless steel needle. Samples were frozen in liquid nitrogen and thawed at 0 °C before spectra were measured. The temperature was held constant (±0.1 °C) by immersion of the Schlenk tube in a Lauda (RC-6) constant temperature water bath.

Rate constants, k_{obs}, were determined by monitoring decreasing and increasing IR absorbances (A_{obs}) of the most intense bands of the reactant and product, respectively. Convenient temperature ranges were selected for each ligand, and at least six runs were carried out over a 20−25 °C temperature range. Rate constants for air-stable compounds were determined by fitting absorbance data to single-exponential curves using GraFit (ver. 3.09b) data analysis software. For air-sensitive ligands, rate constants were obtained from the slopes of $\ln(A_{obs} - A_\infty)$ vs time plots for decreasing absorbances or $\ln(A_\infty - A_{obs})$ vs time plots for increasing absorbances. Kinetic measurements were usually followed over four half-lives. Activation parameters were obtained by unweighted linear least-squares analysis of the dependence of $\ln(k_{obs}/T)$ on $1/T$,[16] and the standard error in k ($\sigma(k_{obs})$%) was determined from the scatter of the values of $\ln(k_{obs}/T)$ around the linear Eyring plot.

The rate of formation of the monodentate complexes **1(a−g)** from $Ru(CO)_4(C_2H_4)$ was much faster than the subsequent ring closure reactions. However, the formation of **1h** (P−P = dpp-benzene) was sufficiently slow, compared with the rate of chelation, for it to be necessary to use a more labile alkene in place of ethylene in order to facilitate the formation of the η^1-(P−P) complex. The bulky 1-butene is known to dissociate considerably faster from $Fe(CO)_4$(alkene) than the ethylene complex.[17] This proved to be so for the $Ru(CO)_4$(alkene) complexes as well so that $Ru(CO)_4(\eta^1$-(dpp-benzene)) could be produced in situ without appreciable chelation before spectroscopic measurements were recorded.

Preparation and Crystallization of $Ru(CO)_3(\eta^2$-$(Ph_2PCH_2CH_2PPh_2)$) (2b). High-pressure reactions were carried out in a 250 mL Parr bomb reactor using procedures outlined by Wilkinson et al.[18] The Parr reactor was charged with tririutheniumdodecacarbonyl (160 mg, 0.25 mmol), bis(diphenylphosphino)ethane (300 mg, 0.75 mmol), and benzene (25 mL). The reactor was purged three times with CO gas and pressurized to 94 atm. The reaction mixture was heated to 100 °C for 12 h and was then cooled to room temperature and the pressure subsequently released. Infrared spectroscopy revealed no traces of starting material remaining in solution. The pale yellow solution was transferred quickly to a nitrogen-filled flask, and the volume was reduced under vacuum until a precipitate began to form. The solution was cooled by refrigeration at 5 °C for 12 h when a yellow precipitate formed. The solid was collected by filtration and crystallized from benzene/pentane solution at 5 °C. IR ν(CO) in *n*-heptane: 2011 (100), 1945 (77), 1923 (92) cm^{-1} (numbers in parentheses, here and elsewhere are relative absorbances). $^{31}P\{^1H\}$ NMR (C_6D_6): δ ppm 73.5. Solid state ^{31}P MAS $\{^1H\}$ NMR: δ ppm 73.9, 65.5. EIMS: 583 (expected 583).

Preparation and Crystallization of $Ru(CO)_3(\eta^2$-$(Me_2PCH_2CH_2PMe_2)$ (2e). Tririutheniumdodecacarbonyl (30 mg 0.047 mmol) was dissolved in *n*-heptane (150 mL). The solution was bubbled with ethylene gas for 20 min and irradiated with a slide projector lamp until the solution was colorless (∼15 min). A solution of bis(dimethylphosphino)ethane (22 mg, 0.066 mmol) in *n*-heptane (1 mL) was quickly added, and the ethylene was removed under vacuum for 2 min. The flask was recharged with 1 atm nitrogen and placed in a water bath at 75 °C for 1 h. Infrared spectroscopy indicated no starting material remaining in the solution. The heptane was removed under vacuum, and the product was redissolved in hexanes. The compound was purified by repeated precipitation, followed by final crystallization from cold hexanes, yielding dark orange crystals. IR ν(CO) in *n*-heptane: 2005 (69), 1934 (62), 1915 (100) cm^{-1}. $^{31}P\{^1H\}$ NMR: δ ppm 43.0. MS: 335 (expected 335).

Preparation and Crystallization of $Ru(CO)_3(\eta^2$-$(o$-$(PPh_2)_2C_6H_4)$) (2h). A Parr reactor was charged with tririutheniumdodecacarbonyl (100 mg, 0.16 mmol) and *o*-bis-(diphenylphosphino)(benzene) (210 mg, 0.47 mmol) in benzene (50 mL). The reactor was purged three times with CO and pressurized to 95 atm. The mixture was stirred at 100 °C for 12 h and cooled, and the pressure was slowly released. The yellow solution was quickly transferred to a dry nitrogen-filled flask. Infrared spectroscopy revealed no traces of starting material. The volume was reduced to approximately 50% under vacuum, and the product was precipitated with hexanes. The precipitate was redissolved in benzene/hexanes, and yellow crystals were grown at 5 °C over a period of 48 h. IR ν(CO) in *n*-heptane: 2012 (100), 1947 (55), 1927 (80) cm^{-1}. $^{31}P\{^1H\}$ NMR (C_6D_6): δ ppm 72.5. MS: 632 (expected 632).

Preparation and Crystallization of $Ru_2(CO)_3(\mu^2$-$PPh_2)$-$(\mu$-$Ph_2PNMePPh_2)(C(O)NMePPh_2)$ (3). A 500 mL flask was charged with tririutheniumdodecacarbonyl (50 mg, 0.08 mmol) and dry *n*-heptane (300 mL). The solution was bubbled with ethylene for 30 min followed by irradiation with a slide projector lamp until the solution turned colorless (∼15 min). Bis(diphenylphosphino)methylamine (96 mg, 0.24 mmol) was added to the clear solution, and the ethylene was quickly removed under vacuum over a period of 5 min. The resulting solution was stirred overnight at 50 °C before being concentrated to 50 mL. IR ν(CO) bands at 2010 (100), 1946 (60), and 1927 (90) cm^{-1} confirmed the presence of $Ru(CO)_3$(dppma), **2g**. The yellow product was precipitated with pentane and washed three times. Attempts to crystallize $Ru(CO)_3$(dppma) by slow diffusion of pentane into a CH_2Cl_2 solution resulted in the slow decomposition of **2g**, forming product **3** over a period of 1 month as yellow crystals suitable for X-ray analysis. IR ν(CO) in CH_2Cl_2: 2057 (28), 1987 (100), 1960 (51), 1921 (23) cm^{-1}. $^{31}P\{^1H\}$ NMR: δ ppm 159.8 (q), 110.5 (q), 96.9 (m), 62.7 (d). MS: 1085 (1141 − 2CO).

Results

Characterization. The monodentate complexes **1(a−h)**, and the corresponding chelate complexes, were characterized by infrared and solution $^{31}P\{^1H\}$ NMR spectroscopy at 25 °C (Tables 1 and 2). Solid state ^{31}P MAS $\{^1H\}$ NMR spectroscopy was performed on **2b** and revealed two peaks at 73.9 and 63.5 ppm (Figure 1).

The chelate compounds undergo slow decomposition in solution under nitrogen and in air, but **2g** exclusively reacts to form **3** in solution. The other chelate complexes decompose to unresolved product mixtures (Scheme 1).

X-ray crystallography was used to elucidate the solid state structures of **2b**, **2e**, **2h**, and **3**, which were isolated in high yields. Data for the crystal structure analysis are given in Table 3. Compound **2b** (Figure 2) exists as a slightly distorted trigonal bipyramid structure with a phosphine bite angle of 82.66(4)°, which is comparable to other complexes with the dppe ligand.[5b,19] Two molecules of benzene crystallized in the lattice. The equatorial−phosphorus equatorial−carbon angles measured 117.87(11)° and 122.80(10)°, and the angle between the axial phosphorus and axial CO ligand is 174.16(10)°. The angles between the equatorial and

(16) Espenson, J. H. *Chemical Kinetics and Reaction Mechanisms*; McGraw-Hill: New York, 1981.
(17) Cardaci, G. *Int. J. Chem. Kinet.* **1973**, *5*, 805.
(18) Sanchez-Delgado, R. A.; Bradley, J. S.; Wilkinson, G. *J. Chem. Soc., Dalton Trans.* **1976**, 399.
(19) Gargulak, J. D.; Berry, A. J.; Noirot, M. D.; Gladfelter, W. L. *J. Am. Chem. Soc.* **1992**, *114*, 8933.

Table 1. Infrared Spectra of $Ru(CO)_4(\eta^1\text{-}(P-P))$ and $Ru(CO)_3(\eta^2\text{-}(P-P))$ in *n*-Heptane[a]

	$Ru(CO)_4(\eta^1\text{-}(P-P))$			$Ru(CO)_3(\eta^2\text{-}(P-P))$		
(P−P)	ν_1	ν_2	ν_3	ν_1	ν_2	ν_3
dppm	2060 (91)	1987 (40)	1957 (100), 1945 (84)	2010 (100)	1945 (76)	1931 (77)
dppe	2061 (79)	1988 (33)	1954 (100), 1947 (92)	2011 (100)	1945 (77)	1924 (92)
dppp	2061 (91)	1987 (34)	1955 (100), 1946 (98)	2014 (57)	1938 (57)	1913 (100)
dppbu	2061 (86)	1987 (40)	1955 (100), 1946 (90)	2010 (43)	1933 (44)	1908 (100)
dmpe	2061 (57)	1986 (24)	1947 (100)	2005 (69)	1934 (62)	1915 (100)
dcpe	2056 (76)	1980 (25)	1939 (100)	1997 (75)	1922 (94)	1904 (100)
dppma	2061 (95)	1988 (44)	1956 (92), 1947 (100)	2010 (100)	1946 (60)	1927 (90)
dpp-benzene	2059 (72)	1988 (89)	1962 (80), 1946 (100)	2012 (100)	1947 (55)	1927 (80)

[a] Relative intensities are in parentheses.

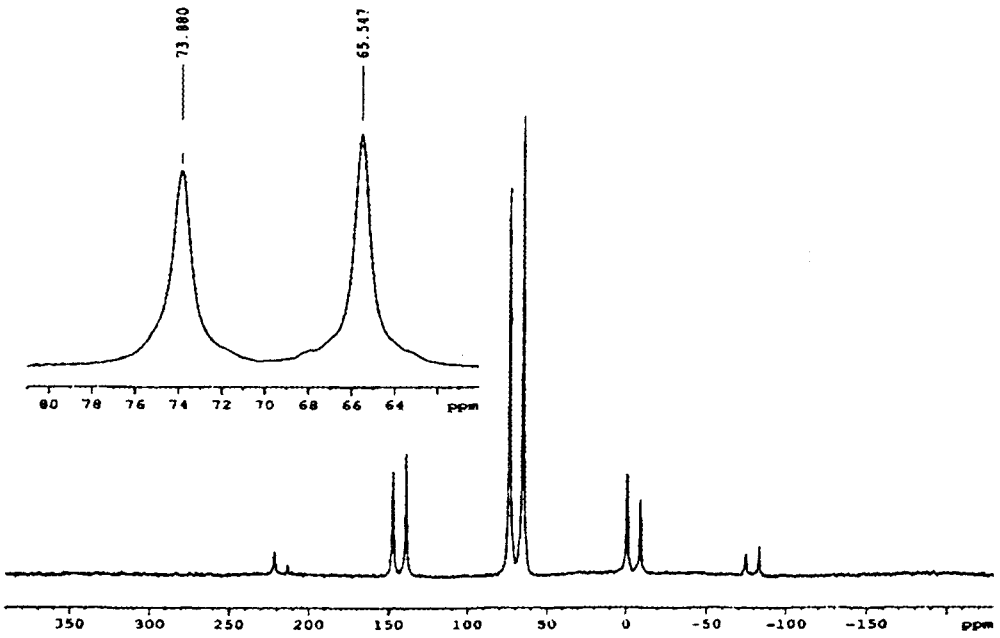

Figure 1. Solid state ^{31}P MAS $\{^1H\}$ NMR spectrum of $Ru(CO)_3$dppe. Inset: Expansion of central doublet.

Table 2. Solution $^{31}P\{^1H\}$ NMR Chemical Shift Data ($\delta^{31}P$ (ppm)) of the Ruthenium Complexes in *n*-Heptane with C_6D_6 Insert

ligand	free ligand	monodentate	chelate
dmpe	−48.4	14.8 (2), −47.0 (2) $J_{pp} = 30$ Hz	43.0
dppe	−12.3	44.9 (2), −12.4 (2) $J_{pp} = 40$ Hz	73.5
dcpe	1.0	54.0 (2), 1.9 (2) $J_{pp} = 36$ Hz	90.5
dppm	−22.0	39.3 (2), −25.7 (2) $J_{pp} = 91$ Hz	−14.2
dppma	73.2	N/A[a]	72.8
dppp	−17.7	39.7 (1), −19.1 (1)	24.1
dppbu	−16.6	40.0 (1), −16.6 (1)	36.2
dpp-benzene	−12.9	N/A[a]	72.5

[a] The rapid rate of chelation reaction and dilute sample concentration prevent measurement of the chemical shift of the monocoordinated complexes.

axial atoms are all near 90°. The complex **2h** (Figure 3) also crystallized as slightly distorted trigonal bipyramids with similar bond lengths and angles (Table 4). The measured Ru−P and Ru−C bond lengths and the P−Ru−P bite angles for **2b**, **2e**, and **2h** all fall within the range for complexes having the molecular fragment $(CO)Ru(\eta^2\text{-}R_2P(CH_2)_2PR_2)$, as indicated by the Cambridge Structure Database.[20]

Compound **2g** slowly converts to **3** in *n*-heptane over a period of several days. X-ray crystallography indicates that **3** is a dimeric ruthenium complex, in which the two Ru atoms are connected by a bridging dppma ligand and a diphenylphosphido unit. The structure incorporates a molecule of hexane cocrystallized in the lattice (Figure 4).

Kinetic Studies. Infrared ν(CO) spectral changes were monitored over the course of reaction as shown in Figure 5. The slow decomposition of the chelate complexes after approximately 80% completion of the reaction was accompanied by the slow decrease in product peak intensity. For **2e**, a shoulder at 1900 cm^{-1} forms as the run progresses. This compound was isolated, but attempts to grow crystals suitable for X-ray crystallography were unsuccessful due to slow product decomposition in solution. No further attempts to purify this compound were undertaken. The A_∞ values for product growth were, therefore, approximated by the highest absorbance value before appreciable peak intensity losses began. First-order rate constants for the growth of product agree with those for disappearance of the monodentate complex. Rate constants are given in Table 5, and their temperature dependence exhibited good Eyring behavior (Figure 6), only the more precise constants obtained from loss of reactant complex being used. Activation parameters are shown in Table 6.

(20) Allen, F. H.; Kennard, O. 3D Search and Research Using the Cambridge Structural Database. *Chem. Des. Automation News* **1993**, *8* (1), 1, 31−37.

Table 3. Crystal Data[a] and Structure Refinement for 2b, 2h, and 3

	2b·2(C_6H_6)	**2h**	**3**·(C_6H_{14})
empirical formula	$C_{41}H_{36}O_3P_2Ru$	$C_{33}H_{24}O_3P_2Ru$	$C_{29}H_{26.50}NO_{2.50}P_2Ru$
fw	739.71	631.53	592.02
temp (K)	150(2)	100.0(1)	150(2) K
cryst syst	triclinic	monoclinic	monoclinic
space group	$P\bar{1}$	$P2(1)/c$	$P2(1)/n$
unit cell dimens	a = 9.478(2) Å	a = 13.5042(4) Å	a = 12.06580(10) Å
	b = 11.899(2) Å	b = 13.4521(4) Å	b = 22.3699(4) Å
	c = 17.596(4) Å	c = 15.8184(5) Å	c = 19.2425(3) Å
	α = 102.10(3)°	α = 90°	α = 90°
	β = 94.25(3)°	β = 99.413(2)°	β = 91.4510(10)°
	γ = 112.73(3)°	γ = 90°	γ = 90°
volume (Å^3)	1762.9(6)	2834.9(10)	5192.09(13)
Z	2	4	8
density(calcd) (Mg/m^3)	1.394	1.480	1.515
abs coeff (mm^{-1})	0.573	0.699	0.757
F(000)	760	1280	2412
cryst size (mm)	0.22 × 0.18 × 0.12	0.15 × 0.12 × 0.10	0.35 × 0.25 × 0.20
θ range for data collection (deg)	4.23−26.41	4.13−26.38	2.48−26.38
no. of reflns collected	7025	19 820	71 475
no. of ind reflns	7025 [R(int) = 0.0000]	5766 [R(int) = 0.043]	10381 [R(int) = 0.056]
no. of data/restraints/params	7025/0/425	5764/0/352	10381/9/639
goodness-of-fit on F^2	1.043	1.096	1.109
final R indices [$I>2\sigma(I)$]	R1 = 0.0393	R1 = 0.0344	R1 = 0.0411
R indices (all data)	wR2 = 0.1079	wR2 = 0.0832	wR2 = 0.1116
largest diff peak (Å^{-3})	0.625	0.566	1.927

[a] The X-ray structure of **2e** has been completed, and the structural parameters are completely comparable to **2b** and **2h**. The complete structural details have been deposited.

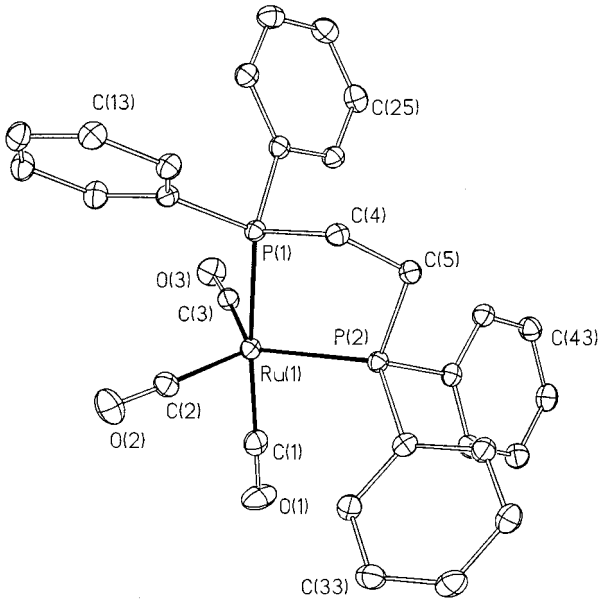

Figure 2. ORTEP view of molecule **2b** with 30% probability ellipsoids. H atoms and the free benzene molecules were omitted for clarity.

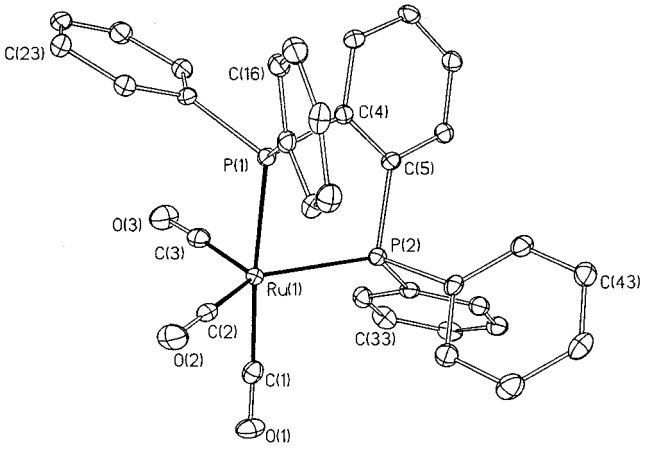

Figure 3. ORTEP view of molecule **2h** with 30% probability ellipsoids. H atoms were omitted for clarity.

Table 4. Selected Bond Angles for 2b, 2h, and 4[a]

	2b	**2h**	**4**
P(1)−Ru(1)−P(2)	82.66(4)	81.31(3)	81.89(3)
C(3)−Ru(1)−P(1)	91.67(11)	89.34(10)	94.57(9)
C(2)−Ru(1)−P(1)	89.81(10)	90.58(10)	91.35(10)
C(3)−Ru(1)−P(2)	122.80(10)	109.33(10)	101.10(9)
C(2)−Ru(1)−P(2)	117.87(11)	129.22(10)	143.49(11)
C(1)−Ru(1)−P(1)	174.20(10)	175.09(9)	163.55(9)

[a] Reference 25.

Discussion

Characterization of Reactants and Products. Formation of the alkene complex from $Ru_3(CO)_{12}$ is quantitative, as shown by the absence of all infrared bands due to the starting material. The rapid displacement of the alkene from $Ru(CO)_4$(alkene) must involve formation of the tetracarbonyl $Ru(CO)_4(\eta^1$-(P−P)), as is the case for substitutions involving monodentate P-donor ligands.[15b] Infrared and $^{31}P\{^1H\}$ spectra are in full agreement with this. The infrared spectra (Table 1) show three-band patterns typical of monosubstituted axial trigonal bipyramid compounds[4a,21] and with one of the bands being broad and usually split. With the exception of dmpe and dcpe, the ν_3 mode is split, usually as a result of slight distortions from C_{3v} symmetry. The former, however, exhibit broad ν_3 stretching modes to account for this loss of symmetry. The spectra show no additional peaks corresponding to equatorially substituted phosphine.[4a] This is usually observed for ligands which are good π-acceptors.[22]

(21) Darensbourg, D. J.; Nelson, H. H.; Hyde, C. L. *Inorg. Chem.* **1974**, *9*, 2135.

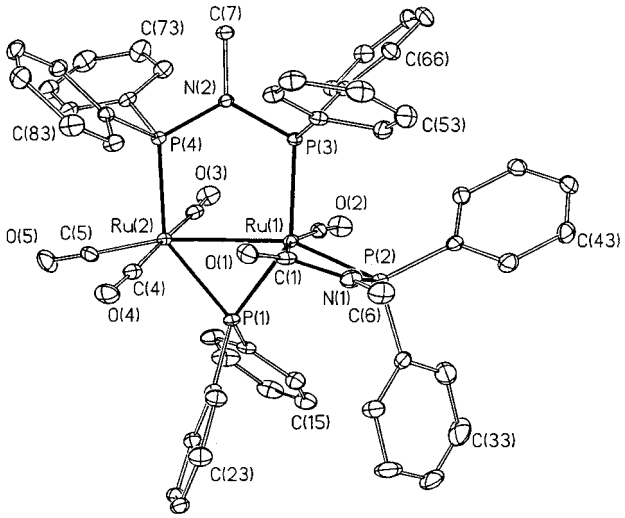

Figure 4. ORTEP view of molecule **3** with 30% probability ellipsoids. The C_6H_{14} molecule and H atoms were omitted for clarity.

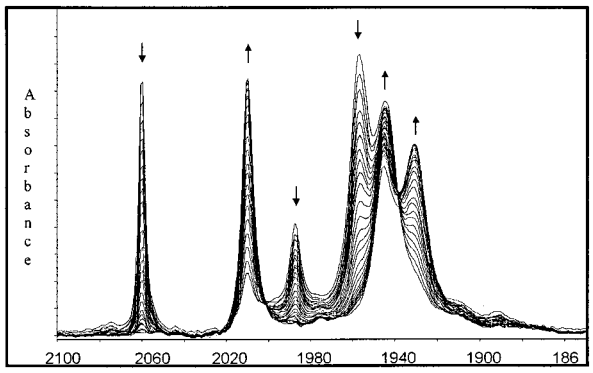

Figure 5. Typical spectral changes for chelation reaction. L = dppm; T = 60 °C. The arrows denote increasing and decreasing absorbances.

Solution $^{31}P\{^1H\}$ NMR spectroscopy (Table 2) of the monodentate complexes exhibits a typical doublet of doublets pattern when the bridging unit contained two carbon atoms or less. Coupling constants between the coordinated phosphorus atom and the free phosphine are 30−91 Hz. The ligands dppp and dppbu show no phosphorus coupling due to the longer alkyl bridge. The monocoordinate complexes of dppma and dpp-benzene were not recorded because the ligand chelated too rapidly for NMR spectroscopy of the tetracarbonyl to be possible. The uncoordinated end of the phosphine ligand typically exhibits a chemical shift very close to that of the free phosphine ligand. The coordinated phosphorus peaks were shifted downfield from the free ligand by 63−53 ppm. Chemical shifts of the coordinated phosphine where n = 1−4 and R = Ph were relatively constant and close to 40 ppm. When n = 1 and 2, P−P coupling constants of 91 and 40 Hz were observed, respectively. The free phosphorus atoms of the ligand still exhibit chemical shifts very close to those of the ligands in free solution. The fact that we observe two distinct phosphorus resonance signals and coupling between the free and coordinated ends of the ligand indicates that the ligand is not undergoing any rapid exchange processes in solution. Infrared and phosphorus NMR spectroscopic data suggest that the monocoordinated complexes are axially substituted trigonal bi-

(22) (a) Martin, L. R.; Einstein, F. W. B.; Pomeroy, R. K. *Inorg. Chem.* **1983**, *22*, 1961. (b) Martin, L. R.; Einstein, F. W. B.; Pomeroy, R. K. *Inorg. Chem.* **1985**, *24*, 2777.

Table 5. Rate Constants[a] for the Chelation Reaction at Various Temperatures in *n*-Heptane

T (K)	$10^4 k_{obs}$ (s^{-1})
dppm	
318.47	1.82
322.58	3.32
327.87	6.08
333.33	10.7
335.57	15.2
337.84	19.7
337.84	20.2
dppe	
322.58	1.28
327.87	2.47
333.33	4.42
335.57	5.46
337.84	8.63
340.14	10.0
342.47	13.7
dppp	
318.47	0.928
323.62	1.71
328.95	3.29 (3.84)[b]
335.57	6.29 (5.66)[b]
338.98	10.8
343.64	21.1 (24.1)[b]
343.64	21.3
dppbu	
322.58	1.64
328.95	4.08
332.23	5.73
337.84	10.3
337.84	10.3
343.64	17.3
343.64	17.8
dmpe	
318.47	0.242[c]
323.62	0.522[c]
327.87	0.930[d]
327.87	0.909[c]
327.87	0.926[e]
333.33	2.04[c]
337.84	3.34[c]
343.64	7.06[c]
343.64	7.32[c]
348.43	1.23[c]
dcpe	
313.48	0.468
318.47	0.886
323.62	1.78
327.87	3.98
333.33	7.93
337.84	13.9
dppma	
284.09	0.689
293.26	2.60
298.51	4.61
303.03	8.64
307.69	15.8
313.48	27.3
dpp-benzene	
277.01	4.30
284.09	15.0
289.02	25.0
293.26	58.9

[a] Only data from reactant loss were used for the Erying analysis. [b] From single-exponential increase of product. [c] [dmpe] = 0.009 M. [d] [dpme] = 0.004 M. [e] [dmpe] = 0.018 M.

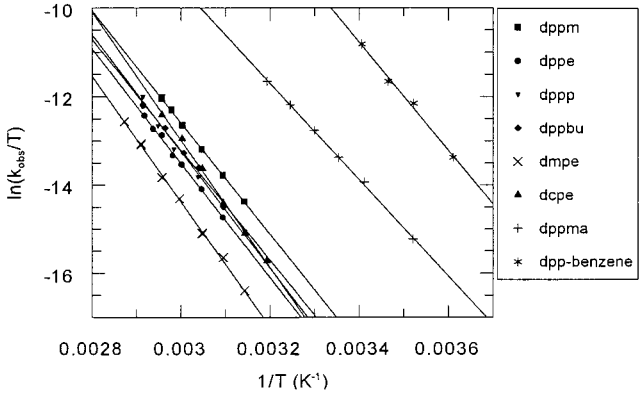

Figure 6. Eyring plots for the chelation reactions.

Table 6. Activation Parameters for the Ring Closure Reaction in *n*-Heptane

ligand	$\Delta H^{\ddagger}$ (kcal mol^{-1})	$\Delta S^{\ddagger}$ (cal mol^{-1} K^{-1})	$10^4\,k_{obs}$ (60 °C)	σk_{obs}[a] (%)
dmpe[b]	28.0 ± 0.3	8.3 ± 1.0	1.86	3.8
dppe[b]	25.7 ± 0.3	3.1 ± 1.5	4.44	
dppbu[b]	25.3 ± 0.4	2.6 ± 1.3	5.75	
dppp[b]	26.1 ± 0.3	5.0 ± 1.0	6.73	
dcpe[b]	28.6 ±0.4	12.8 ± 1.2	7.49	
dppm[b]	25.1 ± 0.4	3.0 ± 1.3	11.2	
dppma[b]	21.0 ± 0.2	−3.2 ± 1.0	242	
dpp-benzene[c]	24.2 ± 1.4	15.0 ± 4.9	9770	13

[a] Standard error of measurement of k_{obs} obtained by the method of pooled variances. All unweighted Eyring analyses implicitly involve the assumption that the values of k_{obs} have a percent uncertainty that is independent of temperature. [b] Errors adjusted according to $\sigma k_{obs} = 3.8\%$. [c] Errors correspond to $\sigma k_{obs} = 13\%$.

pyramids with no evidence of equatorially substituted products.

The solution FTIR spectra of the chelate complexes (Table 1) exhibit three bands of similar intensities as expected for axial−equatorial-substituted bidentate phosphine complexes, but one of the bands is broad and generally split. The ν(CO) values vary only slightly from ligand to ligand. Constraints of the bidentate phosphine bite angles (<90°) help to explain the absence of an equatorial−equatorial binding orientation.[23] Solution $^{31}P\{^1H\}$ NMR spectroscopy (Table 3) of the chelate complexes is characterized by one singlet downfield from the chemical shift of the free ligand. This indicates that these complexes are highly fluctional in solution, possibly via a Berry psudorotation process.[24] Attempts to slow the fluctional process at temperatures as low as −90 °C were unsuccessful. However, solid state $^{31}P\{^1H\}$ NMR (Figure 1) on **2b** clearly shows two phosphorus peaks corresponding to axial and equatorial phosphorus atoms, although their assignments are not possible on the basis of this evidence alone.

The solid phase axial−equatorial structure was confirmed by X-ray crystallography on **2b (**Figure 2), **2e**, and **2h (**Figure 3). Recently, a crystal structure of **2b** was independently solved (**4**) by Gladfelter et al.,[25] but the geometrical orientation of the phosphine ligands was considerably different (Table 4). Gladfelter's structure was described as intermediate between a trigonal bipyramid with axial−equatorial phosphorus and a square pyramid with an apical CO ligand.[25] In attempting to grow crystals of the decomposition product of **2b** in dichloromethane/hexanes, we grew additional crystals of the chelate complex which crystallized in the same space group and still retained its distorted trigonal pyramidal geometric orientation, but no solvent molecules crystallized in the lattice. These results are further evidence of the highly flexible nature of the molecule, which can crystallize in different orientations and crystal lattices, depending on the crystal growing conditions.

Complex **3** (Figure 4) forms from the slow reaction of **2g** in *n*-heptane solution. The mechanism of this transformation is yet unknown, but we suspect it involves initial cleavage of a weak phosphorus−nitrogen bond,[26] followed by attack of the free nitrogen on one of the carbonyl ligands. This activated compound can in turn dimerize with another molecule of **2g** to form **3**. No further study into this process has been undertaken. Otherwise the chelate products $Ru(CO)_3(\eta^2\text{-}(P-P))$ usually decompose slowly in solution and solid state, forming inseparable product mixtures.

Kinetic Analysis. The chelation reactions proceed cleanly in solution, as evidenced by good isobestic points throughout the first 80% of the reaction, and a typical kinetic run is shown in Figure 5. The slow decomposition of the chelate products does not affect our kinetic results since the rate of loss of starting material equals the initial rate of loss of products provided we use estimated values of A_∞ that lie near the maximum absorbance of chelate product before appreciable decomposition takes place. Decreasing absorbances due to reactant complex give excellent fits to single-exponential first-order behavior, and the derived rate constants show no dependence on the concentration of the free ligand as expected for the intramolecular conversion of the ligand from the monodentate to bidentate mode of binding. The rate constants fit well to Eyring plots (Figure 6), and the standard errors of measurement derived from the scatter of the values of $\ln(k_{obs}/T)$ around the least-squares line show that the data are of high precision.

One exception to this is with the ligand dppma because the rate of chelation was comparable to the rate of displacement of the ethylene from the ethylene complex. The very low solubility of dppma in *n*-heptane prevented the use of large excesses of ligand, and we therefore had to fit our data to double-exponential curves, with the second rate constant corresponding to the chelation reaction and the first to the rate of introduction of the dppma. As expected, the reaction rates for chelation were independent of free ligand concentration.

The uncertainty in k_{obs} was calculated by applying the method of pooled variances to all the Eyring analyses.[27] Each value of k_{obs} was weighted according to the assumption of a common percent standard error $\sigma(k_{obs})$ for all complexes irrespective of temperature.[28] The

(23) Dierkes, P.; Van Leeuwen, P. W. N. M. *J. Chem. Soc., Dalton Trans.* **1999**, 1519.
(24) Shriver, D. F.; Atkins, P. W.; Langford, C. H. In *Inorganic Chemistry*, 2nd ed.; W. H. Freeman and Co.: New York, 1994; Chapter 7.
(25) Skoog, S. J.; Jorgenson, A. L.; Campbell, J. P.; Douskey, M. L.; Munson, E.; Gladfelter, W. L. *J. Organomet. Chem.* **1998**, *557*, 13.
(26) Browning, C. S.; Farrar, D. H. *J. Chem. Soc., Dalton Trans.* **1995**, 2005.
(27) Mandel, J. *The Statistical Analysis of Experimental Data*; Interscience: New York, 1964.

error was estimated from $\sigma(k_{obs}) = 100((\sum\Delta^2)/(N-n))^{1/2}$ where $\Delta = (k_{obs} - k_{calc})/k_{calc}$, N = total number of measurements of k_{obs}, n = the total number of parameters obtained from the experiment (two for each Eyring analysis), and the values of k_{calc} are obtained from the least-squares analyses. This method allows for a greater number of degrees of freedom, $N - n$, to be used in the estimates of $\sigma(k_{obs})$, and, therefore, smaller "student's *t*" factors are used to calculate any particular confidence level. The constant percentage uncertainty irrespective of temperature has been shown elsewhere to be generally valid.[29] This is equivalent to assuming a constant absolute error in $\ln(k_{obs}/T)$, an assumption implicit in all unweighted least-squares Eyring analyses. It should be noted that values of Δ for dpp-benzene were not included in the pooled Eyring analysis but were treated separately. The significantly faster rate of reaction lead to a higher standard error than found for the other ligands.

The errors in $\Delta H^{\ddagger}$ and $\Delta S^{\ddagger}$ were calculated from the pooled value of $\sigma(k_{obs})$ and obey "the rule of three",[30] which is based on the fact that the free energies of activation ($\Delta G^{\ddagger}$) have a very small error. Therefore, the error in the enthalpy of activation $\Delta(\Delta H^{\ddagger})$ will be equal to the error in $T\Delta S^{\ddagger}$ ($T\Delta(\Delta S^{\ddagger})$), and $\Delta(\Delta S^{\ddagger})$ will be equal to 1000/T units of $\Delta(\Delta H^{\ddagger})$, or $\sim 3\Delta(\Delta H^{\ddagger})$.[31]

The Intimate Mechanism. Although the stoichiometric mechanism involves the intramolecular displacement of CO from $Ru(CO)_4(\eta^1\text{-}(P-P))$, the question of the extent, if any, of Ru−P bonding in the transition state (i.e., the intimate mechanism) has to be addressed by examining the trends in the activation parameters. The rate constants at 60 °C increase with changing ligand along the series dmpe (0.4) < dppe (1.0) < dpppbu (1.3) < dppp (1.5) < dcpe (1.7) < dppm (2.5) ≪ dppma (54.4) ≪ dpp-benzene (2200). The changes from dmpe to dppm are quite small, and the only major distinction involves dppma and dpp-benzene. However, the relative rates are the result of more significant, but often opposing, changes in $\Delta H^{\ddagger}$ and $T\Delta S^{\ddagger}$ at 60 °C (Table 6). The values of $\Delta H^{\ddagger}$ vary by 9 kcal mol^{-1} and $T\Delta S^{\ddagger}$ by 6 kcal mol^{-1}. The slowest reaction has the highest $\Delta H^{\ddagger}$, whereas the fastest reaction has the most positive $\Delta S^{\ddagger}$ and the second lowest $\Delta H^{\ddagger}$. The relative rates are not, therefore, likely to shed much light on the intimate mechanism of these chelation reactions.

On the other hand, the activation parameters do help us to consider what contribution, if any, from Ru−P bonding there might be in the transition state (Scheme 2). Purely CO dissociative reactions are characterized by $\Delta S^{\ddagger}$ values ~16 cal K^{-1} mol^{-1} or higher.[2] Reactions of $Ru(CO)_4L$ (L = CO or monodentate P-donors) have $\Delta S^{\ddagger}$ values ranging from 12.6 ± 0.6 to 18.3 ± 0.5 cal K^{-1} mol^{-1}, and all react dissociatively.[4a] Only when the bidentate phosphines in $Ru(CO)_4(\eta^1\text{-}(P-P))$ are dcpe and dpp-benzene do the reactions have such positive values of $\Delta S^{\ddagger}$, and we conclude that complexes with these ligands are reacting mainly by a Ru−CO dissociative mechanism. In the case of P−P = dcpe this is likely to be associated with the large size of the C_6H_{11} groups, which must destabilize the ground state toward CO dissociation and disfavor associative attack by the free P-donor atom. This effect must completely override the tendency of the basic entering PCy_2 group to undergo an associative type of reaction. The dissociative nature of the reaction of $Ru(CO)_4$(dpp-benzene) also probably arises from ground state steric effects. The substitution of an ortho-hydrogen by a PPh_2 group in one of the Ph rings of PPh_3 hardly affects the value of $\Delta S^{\ddagger}$ ($\Delta S^{\ddagger}$ for $Ru(CO)_4PPh_3$ = 17.3 ± 0.8 cal K^{-1} mol^{-1}),[4a] but $\Delta H^{\ddagger}$ decreases by almost 6 kcal mol^{-1}. Other large ligands such as PCy_3 and P^tBu_3 also significantly decrease $\Delta H^{\ddagger}$ for CO dissociative reactions on $Ru(CO)_4L$ compared with smaller ligands. The *o*-PPh_2 group in $Ru(CO)_4$(dpp-benzene) is probably oriented away from the Ru center, also for steric reasons (Scheme 3). In fact, the dpp-benzene complex reacts dissociatively at a rate that suggests its effective size is even greater than P^tBu_3.[4a]

Scheme 2. Schematic Depicting Bond Making and Bond Breaking in the Transition States

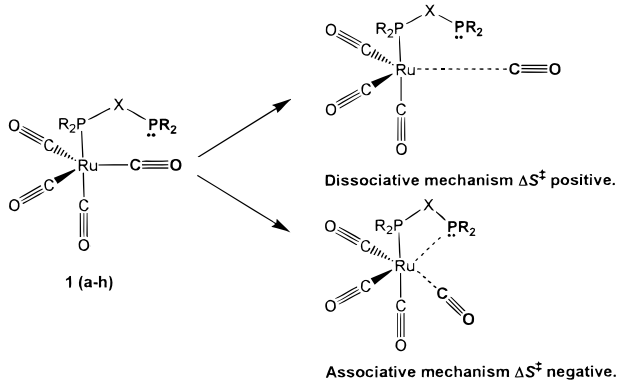

Scheme 3. Geometric Orientations of Chelating Ligands Attacking the Central Ruthenium Atom[a]

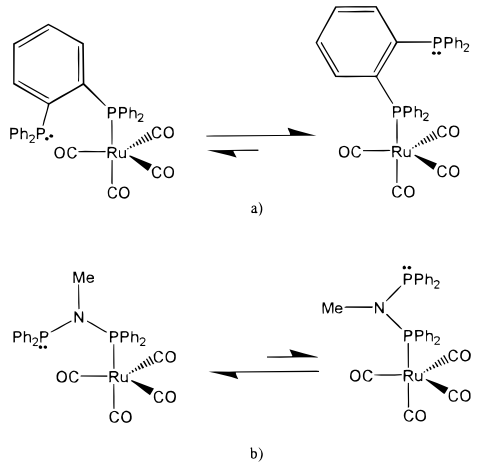

[a] (a) dpp-benzene is sterically crowded, and the free PPh_2 prefers to point away from the metal. (b) dppma is not very large and is capable of positioning the free PPh_2 group near the metal center.

(28) Poë, A. J.; Sekhar, V. C. *Inorg. Chem.* **1985**, *24*, 4376.
(29) (a) Poë, A. J.; Vuik, C. P. J. *J. Chem. Soc., Dalton Trans.* **1972**, 2250. (b) Poë, A. J.; Vuik, C. P. J. *Can. J. Chem.* **1975**, *53*, 1842. (c) Poë, A. J.; Vuik, C. P. J. *Inorg. Chem.* **1980**, *19*, 1771.
(30) Poë A. J. In *Mechanisms of Inorganic and Organometallic Reactions*; Twigg, M. V., Ed.; Plenum Press: New York, 1983; Vol. 8, Chapter 10.
(31) We take this opportunity to demonstrate this phenomenon because of the misinformed view, sometimes expressed, that the extrapolation of Eyring plots to $1/T = 0$ is so long that entropies of activation are extremely imprecise and cannot have any valid use. If $\Delta S^{\ddagger}$ values are obtained from the gradients of the linear plots of $\Delta G^{\ddagger}$ against T (a classical definition of entropy changes), then no "long extrapolation" is involved, yet the value of $\Delta S^{\ddagger}$ and its uncertainty are essentially the same.

This is not surprising in view of the very large ortho substituent on one of the phenyl rings of PPh_3 (Scheme 3).

At the other extreme $Ru(CO)_4(\eta^1$-dppma) seems to react by an appreciably associative intimate mechanism because the value of $\Delta S^‡$ is at least 15 cal K^{-1} mol^{-1} more negative than for a purely dissociative reaction and the value of $\Delta H^‡$ is exceptionally low. Most of the other complexes also have appreciably low values of $\Delta S^‡$, suggesting that they all have significant contributions from Ru−P bond making in the transition state. This Ru−P bond making has to be considered as a description of an "average event" since reactions could occur by mixtures of purely dissociative and associative processes in proportions that change systematically with the nature of the P−P ligand. We can list the reactions in order of increasing associative character as follows: P−P = dpp-benzene < dcpe < dmpe < dppp ≤ dppm ≈ dppbu ≈ dppe ≪ dppma. Apart from the proposed steric effects mentioned above, the order of increasing associative character is not easy to rationalize because of the very nature of the bidentate ligands in $Ru(CO)_4(\eta^1$-(P−P)). The more basic the coordinated P-donor atom is, the more difficult Ru−CO bond breaking might be expected to be,[4a,32] but this effect is probably small.[4a] The corresponding noncoordinated P-donor atom would be expected to be more nucleophillic, but the effect of the bonded P-donor atom could offset this. A mixture of steric and electronic effects would also complicate this already complicated picture. In this case, the ligand that reacts with the most associative character is distinguished by having an N-Me group instead of $(CH_2)_n$ groups joining the two PR_2 ends. This may be due to this ligand's potential to bind to the Ru center in a fashion allowing for close attack of the incoming phosphorus atom (Scheme 3).

A comparison of these results can be made with those of Connor et al. (Table 7)[8] on octahedral complexes of Cr, Mo, and W. On the basis of the values of $\Delta S^‡$, reaction of $Ru(CO)_4(\eta^1$-dmpe) has much less bond making than that of $M(CO)_5(\eta^1$-dmpe) (M = Mo or Cr). On the other hand, $Ru(CO)_4(\eta^1$-dppm) has much more bond making than $Cr(CO)_5(\eta^1$-dppm), which reacts mainly by Cr−CO bond breaking. Reactions of $M(CO)_5(\eta^1$-dppe) (M = Cr, Mo, and W) also exhibit the well-known "triad effect".[3]

(32) Sowa, J. R.; Angelici, R. J. *Inorg. Chem.* **1991**, *30*, 3534.

Table 7. Activation Parameters for the Chelation Reactions of $M(CO)_5(\eta^1$-(P−P))[a]

M	P−P	$\Delta H^‡$ (kcal mol^{-1})	$\Delta S^‡$ (cal mol^{-1} K^{-1})
Cr	dmpe	31	1.5
	dppm	34	17
	dppe	32	6.4
	dcpe	35	9.2
Mo	dmpe	28	−1.7
	dppe	28	3.3
	dcpe	31	8.1
W	dppe	37	9.5

[a] Reference 8.

Conclusion

Chelation kinetics of a variety of bidentate phosphine ligands have been studied for a number of five-coordinate $Ru(CO)_4(\eta^1$-(P−P)) complexes. Entropies of activation range from −3.2 to 15 cal mol^{-1} K^{-1} and indicate a broad range of bond making vs bond breaking in the transition states. Volumes of activation ($\Delta V^‡$) are, unfortunately, not available, but there are difficulties associated with such reactions involving phosphorus donors. The UV−vis absorbance changes, which usually have to be monitored rather than FTIR when reactions under high pressures are followed, are very small. Van Eldik et al.[9] have measured the kinetics of ring closure reactions involving bidentate nitrogen donors in complexes where absorbance changes are considerably larger, and they found a positive correlation between values of $\Delta S^‡$ and $\Delta V^‡$. We therefore believe that we can rely on our $\Delta S^‡$ values as providing a reliable insight into the intimate mechanisms of chelation, but a detailed rationalization of the observed trends is harder to find because of conflicting effects of changing donor and free P atoms in the $Ru(CO)_4(\eta^1$-(P−P)) complexes.

Acknowledgment. We wish to thank the University of Toronto and the Natural Sciences and Engineering Research Council, Canada, for financial support, and Digital Specialty Chemicals for the donation of phosphorus ligands. Dr. Alex Young is thanked for making mass spectroscopic measurements.

Supporting Information Available: Tables of crystallographic parameters, positional and thermal parameters, and complete bond distances and angles of **2b**, **2e**, **2h**, and **3**. This material is available free of charge via the Internet at http://pubs.acs.org.

OM000289T